International Journal of Natural and Engineering Sciences
E-ISSN: 2146-0086 19(1): 1-9, 2025
Research Article

Structural And Magneto Absorption Study of Hard and Soft Ferrite

Usha Praveena V J[1, a]*, A.Rajani Malathi[2,b]

[1]*Department of Physics, St. Francis College for Women, Hyderabad, Telangana, 500 016, India*
[2] *Department of Physics, Osmania University, Hyderabad,Telangana, 500 007, India.*

*Corresponding author: : usha.praveena@sfc.ac.in

(Received: 22 June 2023 / Accepted: 19 February 2025)

a: ORCID 0000-0002-8811-5472, b: ORCID 0000-0003-2626-0436

Abstract

This present study reports structural features and magneto absorption properties of Ba and Ni-Zn ferrite nanoparticles with a composition of $BaFe_{12}O_{19}$ and $NiZnFe_4O_4$.The structural properties of the samples were studied using X-ray powder diffraction (XRD), Scanning electron microscopy (SEM). The XRD patterns of samples show crystalline peaks owing to ferrite presence. The SEM image shows the collection of nanoparticles with empty spaces. The magnetic characteristics of nanoparticle samples were examined using a vibrating sample magnetometer (VSM). Broad band magnetic resonance in polycrystalline samples were measured at room temperature and frequency (f=1−18GHz) ranges of microwave magnetic field availing ENA vector network analyzer and a copper strip coil that contains one of the samples mentioned above. With an increase in microwave signal's frequency, so does the increment in critical field value. Plot study of acquired graph indicates that Ferromagnetic resonance (FMR) is responsible for the peculiarities in magneto absorption that have been observed.

Keywords: Barium ferrite, nickel zinc ferrite, x ray powder diffraction, network analyzer, magnetic resonance

Introduction

Hexaferrites, which have anisotropy fields two to three orders of magnitude higher than spinels, are commonly utilized. These include pure and substituted barium ferrites and nickel zinc ferrites [1-4]. These compositionally modified hexaferrites operate at frequencies ranging from 2 to 18 GHz. Due to their high coercive field and saturation magnetization (H_c~325−400kAm^{-1}, M_s~280−350kAm^{-1}), these are utilized in magnetic recording and permanent magnet fabrication. Notable examples are $BaFe_{12}O_{19}$ and $NiZnFe_4O_4$, both categorized as "M-type hexaferrite" with uniaxial magnetic anisotropy along the crystallographic c-axis. In recent years, barium ferrite has garnered significant interest as a ferric-magnetic material ascribed to its magnificent chemical stability and resistance to erosion. Its remarkable anisotropic properties make it a popular choice for production of magnetic and magneto-optic devices [5,6]. Additionally, its high resistivity and permittivity at high frequencies have led to its utilization in microwave devices. Additionally, Nickel zinc ferrite (NZFO) is employed in applications requiring high permeability, such as inductors and EM wave absorbers. Current research focuses on studying nanosized BFO and NZFO particles to minimize energy losses associated with bulk powders [7,8].

The samples were prepared by Solid state reaction method. Structural features were studied using X-ray powder diffraction (XRD) and Scanning electron microscopy (SEM). Elemental composition is found from EDS. The hysteresis M-H loops at room temperature for the samples was obtained using the Vibrating Sample Magnetometer (VSM).A captivating but relatively underexplored characteristic of ferrite oxides is their magnetic field-dependent microwave absorption (MWA). Existing studies suggest that certain members of this oxide family exhibit higher sensitivity to microwave absorption in comparison to DC electrical resistance when subjected to outer magnetic fields, especially near transition from paramagnetic to ferromagnetic states. About 60 % change in microwave resistance in polycrystalline manganites with a small magnetic field of *H*~ 500Oe was reported by Owens [9], higher change (~90%) for similar field strength in

powder sample was reported by Srinivasu *et al* [10], but smaller magneto absorption ~20% for H = 10kOe in thin film was reported by Tyagi *et al*[11].

At the point when the frequency of incoming microwave attractive field corresponds with the precessional frequency of magnetization, the maximum amount of microwave absorption (MWA) is detected [12]. Furthermore, microwave retention will happen even without a trace of an outside attractive field, domain magnetization processes or magnetoresistance in a ferromagnetic sample is responsible further leading to non-resonant microwave absorption at much lower fields. In most of the existing studies, MWA spectra were recorded using a materialistic electron spin resonance (ESR) spectrometer, with an attractive DC magnetic field swept with a fixed frequency (~10 GHz) determined by the original frequency of resonant chamber [13-15]. Some reports explored recurrence cleared MWA in no outer attractive field in manganite tests utilizing a vector network analyzer (VNA) and explicitly planned transmission line or shorted coaxial links [16-21]. Nevertheless, these studies did not investigate broad-band MWA in the existence of a magnetic field, and there is no prior research on broad-band MWA in the paramagnetic state of manganites [22]. Findings on microwave magneto absorption (MWMA) observed in ferromagnetic samples across a wide frequency spectrum (1-18 GHz) are presented. This was accomplished by using ENA Vector Network Analyzer and a copper strip loop, where the strip curl capabilities both as a transmitter to produce the microwave field and as a beneficiary to distinguish the material's high-recurrence attractive reaction.

Materials and Methods

Chemicals and Materials

Barium ferrite and nickel Zinc ferrite Polycrystalline samples were prepared by conventional solid-state reaction method and reported elsewhere.

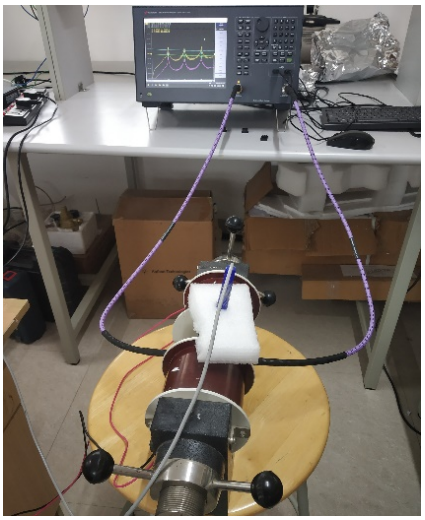

Figure 1. *ENA Vector Network Analyzer*

Test powders were portrayed utilizing X-ray diffractometer (XRD, Philips PW-1730 with Cu-K_α radiation and λ= 1.5406 A°) at room temperature at an examining pace of 2°/min. Microstructural and surface morphological investigations of the examples were completed utilizing SEM of model ZEISS EVO18(special edition). The elemental composition of the samples was obtained by energy dispersive X ray spectrometry. Magnetization of samples were measured using a Vibrating sample magnetometer. (VSM, Model DMS 1660 model) at room temperature. The hysteresis plot gives the connection between the charge M and the applied field H. The boundaries removed from the hysteresis circle that are most frequently used to describe the attractive properties of attractive media incorporate; saturation magnetization M_s, the remanence M_r, the coercivity H_c.

For Microwave magneto absorption study, samples were made into roundabout pellets with aspects of 3 mm diameter and 1.5 mm thickness. A cubical moulded strip loop of comparative aspects was produced using a copper sheet of 0.3 mm thickness displayed in Figure1. The test was immovably squeezed inside strip loop

and internal surface of curl was likewise capped by a slim layer of tape to protect the Copper loop against contacting the test. Two finishes of the curl were associated with ENA (E50063A) utilizing a connector and radio frequency (RF) links. The ENA sources the microwave capacity to the copper strip and measures the reflected capacity to a similar port. An electromagnet was utilized to glide dc attractive field (H_{dc}). Attractive field reliance of microwave power retention has been estimated as far as S11 dissipating boundary of the EM wave reflected from the heap upon change in microwave property of the example by clearing dc attractive field. The ENA estimates the extent of the S11 boundary concerning decibels (dB). Field subordinate of microwave power ingestion (dP/dH) as a component of attractive field at RT can be found.

Results and Discussion

X-ray Diffraction (XRD)

XRD designs for barium ferrite and nickel Zinc ferrite polycrystalline examples show translucent tops because of the presence of ferrite [23]. Moreover, single phase formation of samples is also evident. The XRD patterns were indexed and presented in the Figure 2(a & b).

The Average grain size found to be less than 100 nm, calculated using Debye – Scherrer's equation given below [24]

$$D = 0.9 \lambda / \beta \cos\theta$$

Equation 1

Where 'λ' is wave length of X- ray beam = 1.5406 A°, 'β' is full width at half maxima, 'θ' is Bragg's inclination

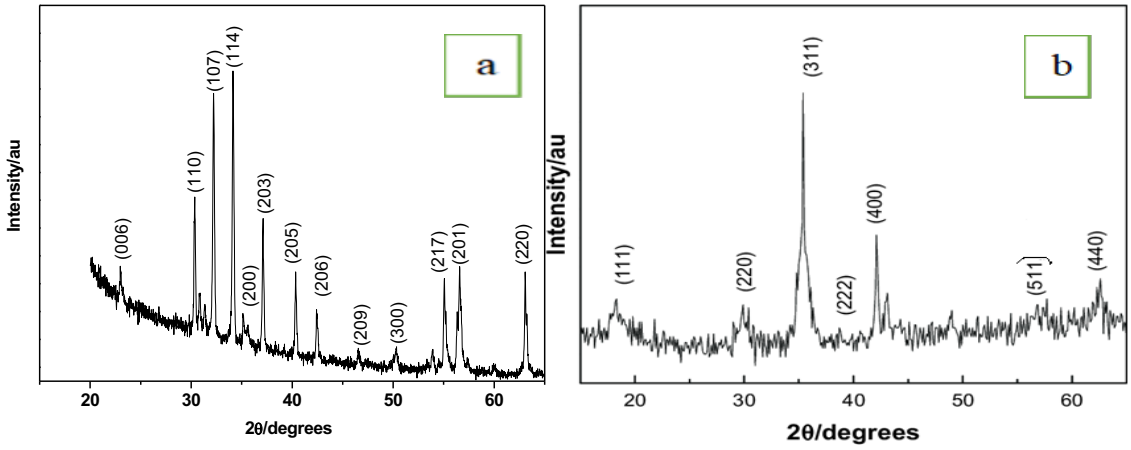

Figure 2. X ray diffraction pattern of (a) Barium ferrite (b) Nickel zinc ferrite

Scanning Electron Microscopy (SEM)

Figure 3(a & b) shows SEM images of prepared Barium ferrite and Nickel zinc ferrite samples. The particles are unpredictable in shape with conservative course of action. In certain particles agglomerates are additionally noticed [25]. It tends to be seen in pictures that the typical grain sizes of the samples are approximately 60 - 80 nm.

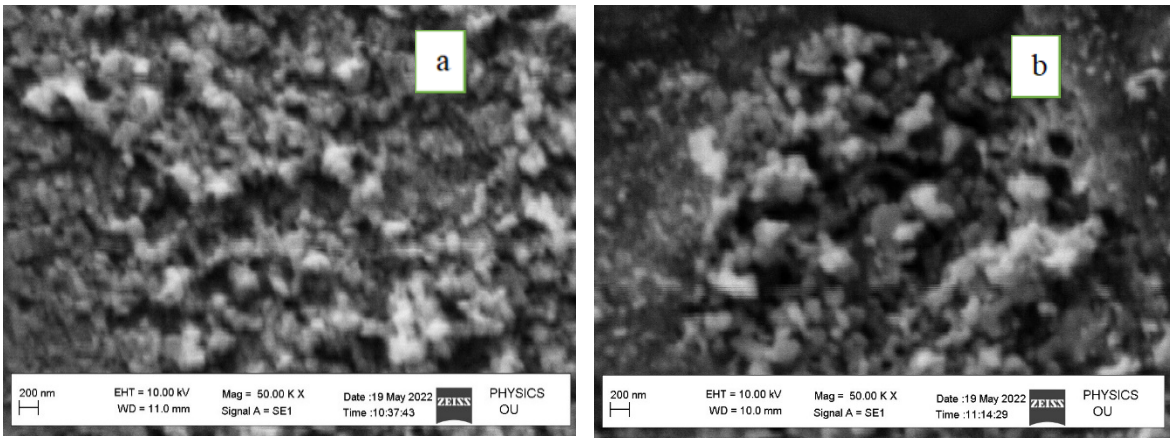

Figure 3. *SEM images of (a)Barium Ferrite and (b)Nickle Zinc ferrite*

Energy Dispersive X-Ray Spectroscopy (EDS)

This study was also carried out to better understand the element distribution in the samples as shown in Figure 4 (a & b). Table 1&2 demonstrates the elemental percentage of each element confirming its presence.

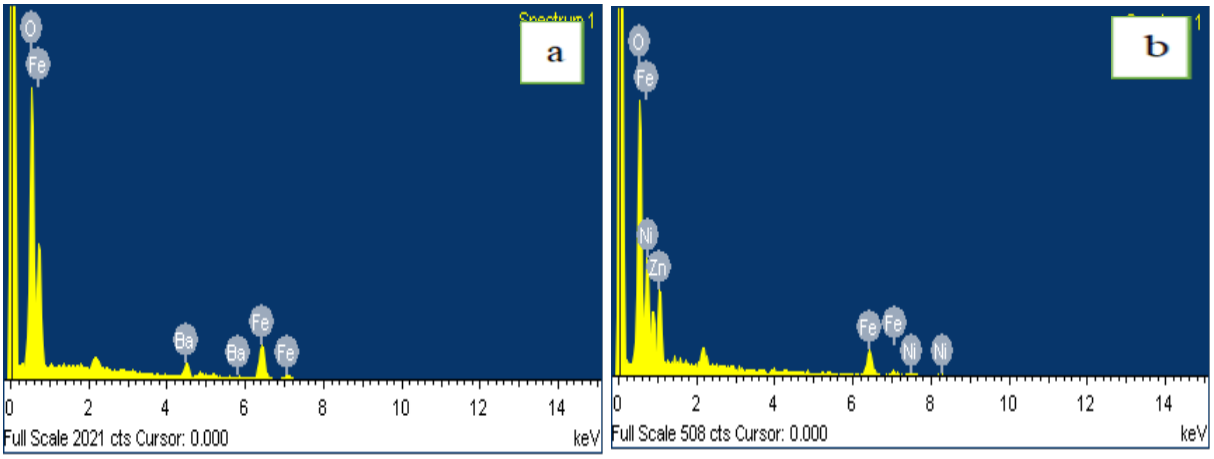

Figure 4. *EDS of(a)Barium Ferrite and (b)Nickle Zinc ferrite*

***Table* 1.** Weight and atomic percentages of Barium ferrite from EDS analysis

Element	Weight (%)	Atomic (%)
Barium	15.25	4.07
Iron	60.10	39.46
Oxygen	24.64	56.47

Table 2. *Weight and atomic percentages of Nickel zinc ferrite from EDS analysis*

Element	Weight (%)	Atomic (%)
Nickel	19.00	11.81
Zinc	13.36	7.46
Iron	45.19	29.53
Oxygen	22.45	51.20

Magnetic Studies (VSM)

Magnetic parameters for samples were found by utilizing a vibrating sample magnetometer at room temperature at a most extreme applied field of 20KOe. Figure 5(a &b) shows the magnetic hysteresis curves of Barium ferrite and Nickel zinc ferrite with given magnetic field at RT. Saturation magnetisation, remanence magnetisation and coercivity were determined from the hysteresis loop and were found to be 30.61emu/gm, 16.16 emu/gm and 623.04 KOe, respectively for Barium ferrite and 17.5 emu/gm, 3.19 emu/gm and 0.794 KOe for nickel zinc ferrite. The hysteresis plots are utilized to check the distinction between soft magnetic materials and the hard magnetic materials [26]. For a hard magnetic material, the region inside the hysteresis circle ought to be enormous on the grounds that it addresses how much helpful attractive energy that can be made accessible to take care of business. However,

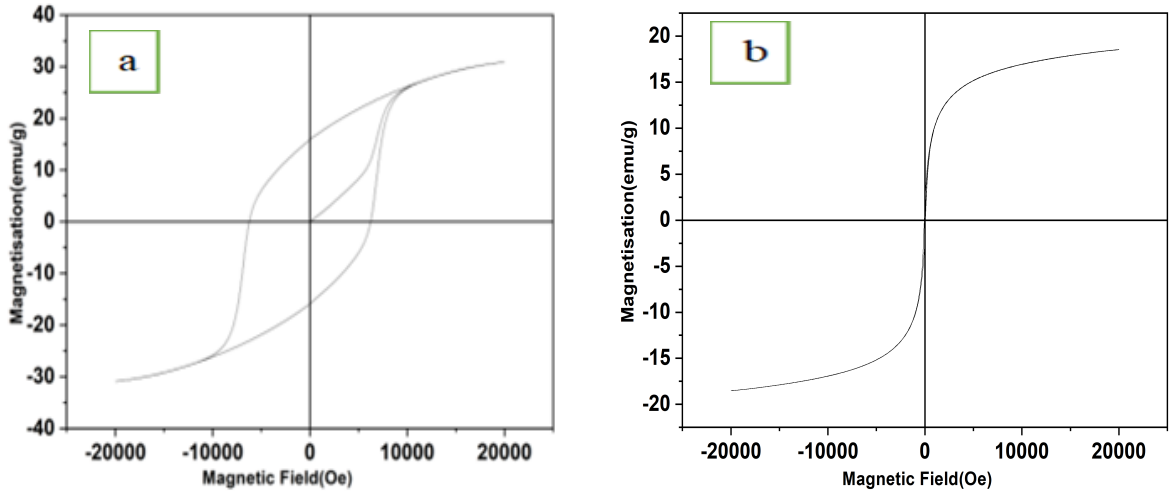

Figure 5. *Magnetic hysteresis loops of (a) Barium ferrite and (b) Nickel zinc ferrite at room temperature*

for a soft magnetic material, it addresses unfortunate center flaws. Materials having properties among hard and soft materials are alluded to as semi-hard magnetic materials.

Microwave magneto absorption studies (MWMA)

Ferromagnetism in ferrites is understood to arise from the double exchange interaction between ferrite ions. The combined spins of the core and electron in Fe particles assume a huge part in deciding the sample's general magnetization. In the setup we used for our measurements, the microwave (MW) traveling through strip loop generates a magnetic field (H_{field}) along the coil's axis and consequently through the sample. The MW magnetic field (H_{field}) and direct

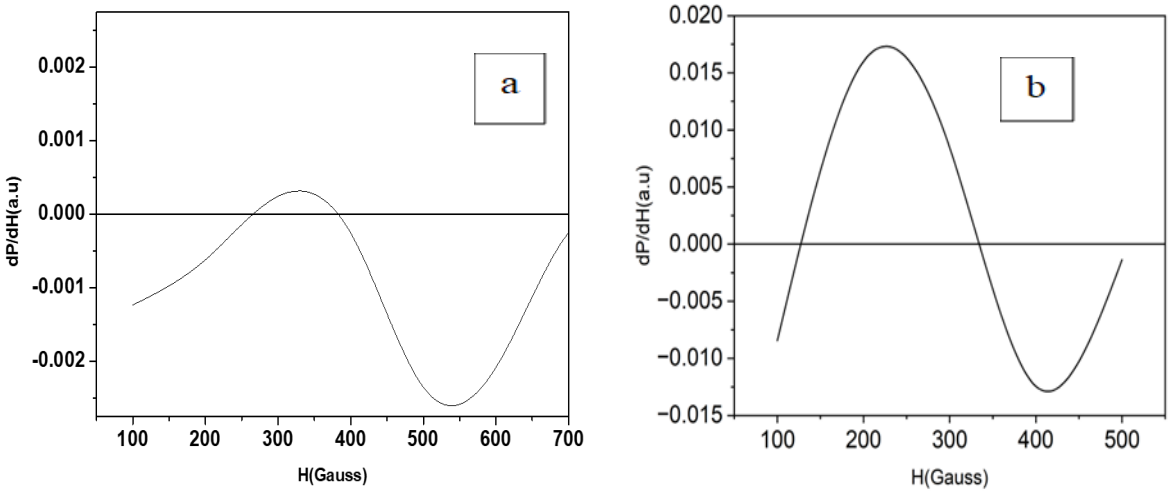

Figure 6. *dP/dH of (a) Barium ferrite and (b) Nickel zinc ferrite*

current magnetic field (H_{dc}) applied will be perpendicular to one another. Consequently, the magnetization experiences a precessional motion around the effective magnetic field (Heff), formed by the combination of the anisotropy field (H_f) and H_{dc}. A full retention happens at the point when the recurrence of the MW attractive field coordinates with the recurrence of charge accuracy. This occurence is called FMR of a ferromagnetic sample [27]. When the system is in resonance, the ferromagnetic sample absorbs the highest amount of power from the microwave (MW) field. We conducted measurements of broadband ferromagnetic resonance (FMR) spectra over a range of frequencies (f = 1−18 GHz) at specific direct current magnetic field strengths [28-34]. Additionally, we gathered dP/dH spectra, varying the direct current magnetic field for specific frequencies within the ferromagnetic regions. Previous studies have indicated that the broadening of the ferromagnetic resonance (FMR) line happens at low frequencies because of nonuniform magnetization circulation or spatial inhomogeneities in the magnetic properties, other than field vacillations and attractive clamor. Plots are displayed in Figure 5(a & b).

Conclusion

The investigations were performed on polycrystalline samples of Barium ferrite and Nickel zinc ferrite prepared via Solid state reaction method. Samples were portrayed morphologically by X-ray beam diffraction spectra and Examining electron microscopy. Single phase of respective samples was affirmed by XRD. The particles are unpredictable in shape with smaller course of action. XRD allowed us to determine the crystalline structure, and SEM provided critical information on surface features, validating a comprehensive characterization.The presence of an attractive hysteresis circle at room temperature fills in as affirmation of the presence of attractive requesting in this sample at ambient conditions. During the application of the strip-coil method for magneto absorption studies, it was ensured that the resonant frequency of the empty coil was distinct from the frequencies under investigation. Consequently, this method proves to be effective for exploring magnetization dynamics, not only in insulators as demonstrated previously but also in conducting materials. The substantial changes observed in the samples could hold

considerable importance for sensor applications. To adress future research, ferrite materials with improved magnetic properties, such as higher anisotropy fields or enhanced magnetic moments can be investigated and also sample preparation methods to produce high-quality, single-phase ferrite samples can be considered.

Acknowledgement

One of the author Usha Praveena V J wishes to acknowledge the Management of St. Francis College for Women for supporting the work under SFC-MRP scheme.

References

1. Chandamma N, Manohara BM, Ujjinappa BS, Shankarmurthy GJ, Kumar MS. (2017). Structural and electrical properties of Zinc doped Nickel ferrites nanoparticles prepared via facile combustion technique. *Journal of alloys and compounds*, *702*, 479-488.
2. Raju P, Murthy SR. (2013). Preparation and characterization of Ni–Zn ferrite+ polymer nanocomposites using mechanical milling method. *Applied Nanoscience*, *3*, 469-475.
3. Valko L, Bucek P, Dosoudil R, Usakova M. (2003). Magnetic properties of ferrite-polymer composites. *Journal of Electrical Engineering-Bratislava-*, *54*(3/4), 100-103.
4. Sanida A, Stavropoulos S, Speliotis T, Psarras GC. (2018). Magneto-dielectric behaviour of M-type hexaferrite/polymer nanocomposites. *Materials*, *11*(12), 2551.
5. Chanda A, Chaudhuri U, Mahendiran R. (2020). Microwave magnetoabsorption in R0. 6Sr0. 4MnO3 (R= Pr and Nd). *Journal of Physics D: Applied Physics*, *53*(21), 215004.
6. Nowosielski R, Babilas R, Wrona, J. (2007). Microstructure and magnetic properties of commercial barium ferrite powders. *Journal of Achievements in Materials and Manufacturing Engineering*, *20*(1-2), 307-310.
7. Bhavikatti AM, Kulkarni S, Lagashetty A. (2010). Characterization and electromagnetic studies of nano-sized barium ferrite. *Int. J. Engg. Sci. & Tech*, *2*(11), 6532-6539.
8. Rao CNR. (1999). Novel materials, materials design and synthetic strategies: recent advances and new directions. *Journal of Materials Chemistry*, *9*(1), 1-14.
9. Owens FJ. (1997). Giant magneto radio frequency absorption in magneto-resistive materials La 0.7 (Sr, Ca) 0.3 MnO 3. *Journal of applied physics*, *82*(6), 3054-3057.
10. Srinivasu VV, Lofland SE, Bhagat SM, Ghosh K, Tyagi S. (1999). Temperature and field dependence of microwave losses in manganite powders. *Journal of applied physics*, *86*(2), 1067-1072.
11. Tyagi SD, Lofland SE, Dominguez M, Bhagat SM, Kwon C, Robson MC, Venkatesan T. (1996). Low-field microwave magnetoabsorption in manganites. *Applied physics letters*, *68*(20), 2893-2895.
12. Golosovsky M, Monod P, Muduli PK, Budhani RC. (2012). Low-field microwave absorption in epitaxial La 0.7 Sr 0.3 MnO 3 films that results from the angle-tuned ferromagnetic resonance in the multidomain state. *Physical Review B*, *85*(18), 184418.
13. Shames AI, Auslender M, Rozenberg E. (2009). La-and Mn-sites deficient LaMnO3 as a model system for studying paramagnetic magnetic correlations and spin dynamics in doped manganites. *Journal of Physics D: Applied Physics*, *42*(24), 245002.
14. Angappane S, Rangarajan G, Sethupathi K. (2003). Magnetic clusters in Nd 1− x Sr x MnO 3 (0.3⩽ x⩽ 0.5): An electron-spin resonance study. *Journal of applied physics*, *93*(10), 8334-8336.
15. Joshi JP, Sarathy KV, Sood AK, Bhat SV, Rao CNR. (2004). An electron paramagnetic resonance study of electron–hole asymmetry in charge ordered $Pr_{1-x}CaxMnO_3$ (x= 0.64, 0.36). *Journal of Physics: Condensed Matter*, *16*(16), 2869.

16. Gupta R, Joshi JP, Bhat SV, Sood AK, Rao CNR. (2000). An electron paramagnetic resonance study of Pr0. 6Ca0. 4MnO3 across the charge-ordering transition. *Journal of Physics: Condensed Matter*, *12*(30), 6919.
17. Schwartz A, Scheffler M, Anlage SM. (2000). Determination of the magnetization scaling exponent for single-crystal La 0.8 Sr 0.2 MnO 3 by broadband microwave surface impedance measurements. *Physical Review B*, *61*(2), R870.
18. Li G, Hu GG, Zhou HD, Fan XJ, Li XG. (2001). Absorption of microwaves in La 1− x Sr x MnO 3 manganese powders over a wide bandwidth. *Journal of Applied Physics*, *90*(11), 5512-5514.
19. Cheng YL, Dai JM, Zhu XB, Wu DJ, Yang ZR, Sun YP. (2009). Enhanced microwave absorption properties of intrinsically core/shell structured La 0.6 Sr 0.4 MnO 3 nanoparticles. *Nanoscale research letters*, *4*, 1153-1158.
20. Zhang S, Cao Q. (2012). Electromagnetic and microwave absorption performance of some transition metal doped La0. 7Sr0. 3Mn1− xTMxO3±δ (TM= Fe, Co or Ni). *Materials Science and Engineering: B*, *177*(9), 678-684.
21. Feng X, Wen H, Shen Y. (2013). Microwave absorption properties of Nd0. 7Sr0. 3MnO3 prepared using high-energy ball milling. *Journal of alloys and compounds*, *555*, 145-149.
22. Das R, Chaudhuri U, Chanda A, Mahendiran R. (2020). Broadband electron spin resonance study in a Sr2FeMoO6 double perovskite. *ACS omega*, *5*(28), 17611-17616.
23. Cornell RM, Schwertmann U. (2003). *The iron oxides: structure, properties, reactions, occurrences, and uses* (Vol. 664). Weinheim: Wiley-vch.
24. Klug HP, Alexander LE. (1954). Quantitative Analysis of Powder Mixtures in "X-ray Diffraction Procedures".
25. Praveena U, Kumar VV, Prasad NV, Prasad G, Kumar GS. (2019). Effect of synthesis on properties of Gd doped LaBi5Fe2Ti3O18. *Materials Today: Proceedings*, *11*, 1041-1048.
26. Sánchez Valdés, CF. (2020). Superparamagnetic state in La0. 7Sr0. 3MnO3 thin films obtained by rf-sputtering. *Instituto de Ingeniería y Tecnología*.
27. Rebello A, Naik VB, Mahendiran R. (2009). Huge ac magnetoresistance of La0. 7Sr0. 3MnO3 in subkilogauss magnetic fields. *Journal of Applied Physics*, *106*(7).
28. Pullar RC, Galizia P, Migliano AC, Amaral JS, Galassi C, Carvalho FE. (2023). The ferromagnetic resonance (FMR) of SrZ hexaferrite (Sr3Co2Fe24O41), and the tuning of FMR with an external magnetic field. *Ceramics International*, *49*(14), 24407-24413.
29. Schneider ML, Gerrits T, Kos AB, Silva TJ. (2007). Experimental determination of the inhomogeneous contribution to linewidth in Permalloy films using a time-resolved magneto-optic Kerr effect microprobe. *Journal of Applied Physics*, *102*(5).
30. Nembach HT, Silva TJ, Shaw JM, Schneider ML, Carey MJ, Maat S, Childress JR. (2011). Perpendicular ferromagnetic resonance measurements of damping and Land e′ g− factor in sputtered (Co 2 Mn) 1− x Ge x thin films. *Physical review B*, *84*(5), 054424.
31. Heo JH, You JY, Kang YM. (2022). Synthesis, characterization, and electromagnetic wave absorption properties of Sr3Co2Fe24O41 hexaferrites. *Journal of Magnetism and Magnetic Materials*, *550*, 169051.
32. Arackal S, Nozawa K, Kahmei R, Loi TT, Yabukami S, Shivashankar SA, Sai R. (2022). Resonance frequency above 20 GHz in superparamagnetic NiZn-ferrite. *Applied Physics Letters*, *121*(6).
33. Farhat S, Awad R, Bitar Z. (2024). Comparative study between oxide/soft ferrite, oxide/hard ferrite, and soft/hard ferrite nanocomposites: structural, electrical, and magnetic properties. *Physica Scripta*, *99*(6), 065967.

34. Almessiere MA, Caliskan S, Baykal A, Klygach DS, Trukhanov SV, Slimani Y, Arslan E. (2024). Impact of Ho substitution on structure, magnetic and electromagnetic properties hard-soft nanocomposites. *Materials Science and Engineering: B*, *308*, 117571.